

# Comparative analysis of end wall resistivity in xylem conduits

JOHN S. SPERRY, UWE G. HACKE & JAMES K. WHEELER

Department of Biology, University of Utah, 257S 1400E, Salt Lake City, Utah, 84112, USA

## ABSTRACT

The hydraulic resistivity ( $R$ , pressure gradient/flow rate) through end walls of xylem conduits was estimated in seven species of diverse anatomy and affinity including a vessel-bearing fern, a tracheid-bearing gymnosperm, and angiosperms with versus without vessels. Conduit lengths were measured with a silicone injection method which was easier and more accurate than the usual paint injection. The  $R$  declined linearly with the removal of end walls as stems were shortened from 10 to 0.3 cm. This relationship gave the minimum  $R$  with no end walls present, or the lumen resistivity ( $R_L$ ). This was indistinguishable from the Hagen–Poiseuille value. The maximum  $R$  with all end walls present gave  $R_C$ , the resistivity of end wall and lumen in series. Average end-wall resistivity ( $R_W$ ) was the difference  $R_C - R_L$  and the ‘wall fraction’ was  $R_W/R_C$ . Wall fraction was approximately constant, averaging  $0.54 \pm 0.07$ . This suggests that end wall and lumen resistivities are nearly co-limiting in vascular plants. Average conduit length was proportional to the diameter squared across species ( $r^2 = 0.94$ ). Together with a constant wall fraction, this was consistent with the end wall resistance ( $r_w$ , pressure difference/flow rate) being inversely proportional to conduit length. Lower  $r_w$  in longer conduits is consistent with their having more end wall pits than shorter conduits.

*Key-words:* hydraulic architecture; vessel length; water transport; xylem structure and function; xylem flow resistance.

## INTRODUCTION

The hydraulic resistivity of a xylem conduit ( $R_C$ , pressure gradient/flow rate) is to a first approximation the sum of lumen ( $R_L$ ) and end wall resistivities ( $R_W$ ) in series. Lumen resistivity is a function of inner conduit diameter and it can be quantified by the Hagen–Poiseuille equation. End wall resistivity is less well understood. A longitudinal file of conduits creates an axial flow path through overlapping ‘end walls’ studded with pits. The resistivity of these end walls is certainly a function of the flow resistance through

the connecting pits as well as the distance between successive end walls. This distance will be a function of the conduit length. Modelling studies predict that the resistance of a single pit will increase with increasing safety from cavitation by air-seeding through pit membranes (Sperry & Hacke 2004), but whether pits are a significant bottleneck depends on their number and also the length of the conduit lumen.

Figure 1 illustrates the question addressed by this paper. It shows how conductivity ( $= 1/R$ ; used in Fig. 1 for illustrative purposes) is influenced by conduit length. A short conduit has end walls close together and potentially less area available for pits in overlapping end walls. The end wall resistance per length (= end wall resistivity) will be high and the conduit will be wall-limited with low conductivity. A long conduit of same diameter has widely spaced end walls and potentially more area for end wall pits. Its end wall resistance per unit length will be low and so its conductivity becomes lumen-limited at the Hagen–Poiseuille value. Where are real plants on this continuum? Are they wall-limited, lumen-limited, or are the two components co-limiting? No systematic survey has been done to answer this question, and the available information is contradictory.

Empirical and theoretical work with tracheid-bearing plants indicates a substantial wall limitation, with 14–84% of total xylem resistivity ( $\% R_W/R_C$ ) residing in end-walls (Schulte & Gibson 1988). High end wall resistivity is perhaps not surprising for tracheids which are limited to generally less than a centimetre in length. However, recent modelling of pit resistance suggests that narrower tracheids may be lumen-limited (Hacke, Sperry & Pittermann 2004). Conclusions from vessel-bearing plants are even more ambiguous. In species with wide-vessels such as grapevine, the measured xylem resistivity can be as low as the Hagen–Poiseuille lumen resistivity, indicating a negligible end wall effect (Zimmermann 1983). The same conclusion was reached by Chiu & Ewers (1993) who found no decrease in resistivity of *Lonicera fragrantissima* as stems were cut shorter and end wall resistances successively removed. However, in most species the Hagen–Poiseuille lumen resistivity is much lower than the measured value (Zimmermann 1983 and literature cited therein; Tyree & Ewers 1991 and literature cited therein; Hargrave *et al.* 1994; Martre, Cochard & Durand 2001), suggesting a significant end wall component.

Correspondence: John S. Sperry. Fax: +1 801 581 4668; e-mail: sperry@biology.utah.edu

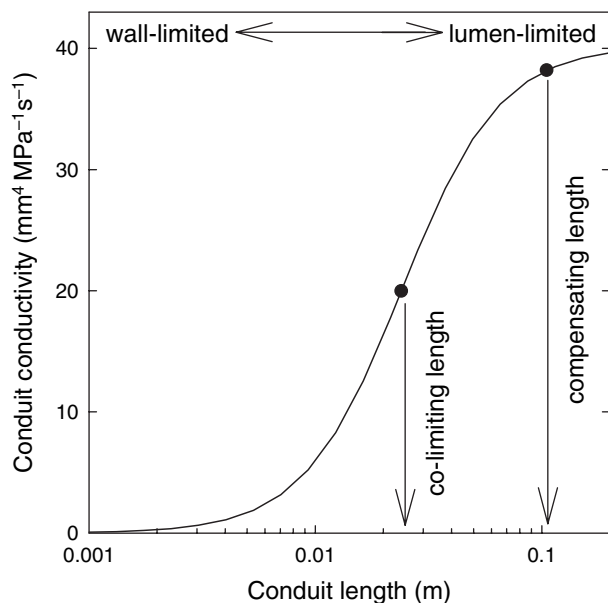


**Figure 1.** Conduit conductivity versus length for a conduit of fixed diameter. Calculation assumes the average lumen conductivity for the vessel-bearing species in the data set, and the observed proportionality of wall resistance ( $r_w$ ) with length ( $r_w \propto 1/L$ ) for the data set. Short conduits are wall-limited with low conductivity, long conduits become lumen-limited at the Hagen–Poiseuille value for the conduit diameter. The co-limiting length corresponds to a 50% end wall resistivity. The compensating length corresponds to 5% end wall resistivity.

A related question is the allometry between conduit diameter and length. As diameter increases, the lumen resistivity declines: the Hagen–Poiseuille equation predicts that  $R_L$  is proportional to  $1/D^4$ . If the end wall resistivity is to maintain the same fraction of the total, it must also decline in the same way:  $R_w \propto 1/D^4$ . As pointed out by Lancashire & Ennos (2002), if the resistance of the end wall ( $r_w$ ) is constant (e.g. the number of pits per end wall is constant), the length between end walls must increase with  $D^4$  to reduce the end wall resistance per unit length and maintain a constant wall fraction. Alternatively if  $r_w$  decreases with increasing conduit wall area (e.g. pits per end wall area is constant,  $r_w \propto 1/LD$ ),  $L$  would only have to increase with  $D^{3/2}$ . Other allometries are conceivable, and whether any is universally applicable is unknown.

In this paper we report the influence of end wall resistivity across seven species ranging from a tracheid-bearing gymnosperm (*Ginkgo biloba* L.) and a vessel-less angiosperm (peppertree, *Pseudowintera colorata* (Raoul) Dandy) to a fern with vessels (bracken, *Pteridium aquilinum* (L.) Kuhn) and angiosperms chosen to bracket a wide range of vessel diameters (grapevine, *Vitis vinifera* L.; boxelder, *Acer negundo* L.; willow, *Salix exigua* Nutt.; elderberry, *Sambucus caerulea* Raf.). We evaluated diameter versus length scaling as well as the relative position of each species in the wall versus lumen-limiting continuum illustrated in Fig. 1. In doing so we also developed improvements in methods and analysis for determining conduit length distributions.

## MATERIALS AND METHODS

### Stem-shortening experiments

If end wall resistivity ( $R_w$ ) is significant, overall xylem resistivity ( $R$ ) will decrease as stems are shortened and end walls removed (Chiu & Ewers 1993). Where possible we used internodes (petioles of bracken) that were at least 10 cm long and measured the resistivity of segments 10, 5, 4, 3, 2, 1, 0.6 and 0.3 cm long. Under measurement conditions (below), stems would have to be cut to less than 0.1 cm before we would expect end effects to decrease the conductivity below Hagen–Poiseuille values (Louden & McCulloh 1999). We expressed the resistivity on a xylem area basis ( $\text{MPa s m}^{-2}$ ) to correct for differences in xylem area. Using internodes minimized complicating effects of side branches. In ginkgo, peppertree, and willow it was not possible to use internodes. For willow and peppertree we used leaf-less stems free of side branches. In ginkgo the long shoots did not have 10 cm long stems without axillary short-shoots. In this species, we cut the short-shoots at their base and sealed the segments with parafilm. Bracken leaves and stems of boxelder and willow were collected from the same plants (clones in willow and bracken) in Red Butte Canyon near the University of Utah in Salt Lake City. Elderberry stems came from the same plant in neighbouring Mill Creek Canyon. Grapevine stems were collected in the senior author's backyard in Salt Lake City from a neighbour's vine. Ginkgo stems were cut from a tree on the University of Utah campus. Peppertree, a vessel-less angiosperm from New Zealand, was collected by Jarmila Pittermann near Auckland, New Zealand and express-mailed to our laboratory at the University of Utah.

Stems were flushed with filtered ( $0.2 \mu\text{m}$ ) 25 mM KCl solution at 100 kPa (plants without torus-margo pits) and 15 kPa (ginkgo with torus-margo pits), respectively, for 30 min to eliminate embolism. Stems were then fitted at one end to a tubing apparatus filled with the same perfusing solution. The other end was immersed in a beaker of solution on an electronic balance (Sartorius, Göttingen, Germany). A background flow rate in the absence of applied pressure was measured gravimetrically before and after measuring the flow rate under pressure (approximately 2–4 kPa) to correct for non-zero flow versus pressure intercepts (Kolb & Sperry 1999). The balance was interfaced with a computer for convenience.

In most species (willow, ginkgo, boxelder, elderberry, peppertree) the resistivity of a given stem length was constant with perfusion time, and so we could measure all lengths (10, 5, 4, 3, 2, 1, 0.6, 0.3 cm) on a single stem. At least 10 stems were measured per species, giving us  $n \geq 10$  measurements at each length. The 0.6 and 0.3 mm long segments were briefly re-flushed at a mild pressure in order to remove any air accidentally introduced during the trimming of these short segments with numerous open vessels. In grapevine and bracken, mucilage tended to cause an increase in resistivity at a given length over time. For these species, we could only measure one or two lengths per stem and more stems were required to achieve 10 or more mea-

surements per stem length. In these species, segments of all length classes were re-flushed for at least 5 min prior to the conductivity measurement at each length. All measurements were adjusted to 20 °C to standardize for the change in viscosity with fluid temperature. Acid fuchsin (0.05% w/w) perfusions were performed to insure that no water was flowing through the pith or other anomalous pathways in the shorter lengths.

### Conduit length distributions

To determine the proportion of open vessels in stem segments of different lengths we measured the vessel-length distribution of stems of similar size and identical origin as used in the shortening experiments. In preliminary experiments we injected the standard paint suspension (1 : 100 pigment : water by weight) into flushed stems to fill up the open conduits (Zimmermann & Jeje 1981; Ewers & Fisher 1989). These stems were then cut at different lengths from the injected surface and the density of paint-filled vessels (number of filled vessels per xylem area) counted. This count was then converted into a vessel-length distribution (see below). However, as reported in the Results section (Table 1), some of the resulting vessel length distributions seemed suspiciously short (e.g. mean vessel length in willow according to the paint method was only 0.4 cm) – presumably because of clogging of paint particles (Tyree, Cochard & Cruziat 2003). We also found it difficult to identify paint-filled vessels with certainty because the paint usually did not fill the entire lumen even after a week of injection at approximately 0.1 MPa of pressure.

As a result of these issues we tried silicone (Rhodorsil RTV-141; Rhodia USA, Cranbury, NJ, USA; imported by Walco Materials, Escondido, CA, USA), which was injected into one end of a flushed stem under pressure (typically 0.2 MPa). This was the same two-component silicone elastomer used for vessel casting (André 1998). The colourless silicone was mixed with a red pigment paste (Silastic LSPRD11; Dow Corning, Kendallville, IN, USA) to make it visible in section. Stems (35–50 cm long) were injected for 24 h using a custom-made pressure chamber. The injection pressure was kept constant during this period. We have

**Table 1** Comparison of mean vessel lengths calculated from stems injected with paint pigment solution versus silicone

Species	Paint		Silicone		P-value
	mean (m)	SD (m)	mean (m)	SD (m)	
Elderberry	0.011	0.0035	0.031	0.0061	0.059
Willow	0.004	0.0004	0.015	0.0046	0.044
Boxelder	0.019	0.0034	0.022	0.0035	0.505
Grapevine	0.0573	0.0030	0.128	0.0485	0.331

SD, standard deviation; P, probability values for *t*-test comparison. The lower the probability, the more likely the two means are different. Means are from log-transformed length distributions,  $n = 3-5$  stems.

subsequently found that an injection period of 2 h followed by a brief period (approximately 30 min) of drying in an oven at 70 °C yields identical results (U.G. Hacke, unpubl.). After the silicone had cured, stems were sectioned for analysis. Cross-sections were observed using a fluorescence microscope, a charge-coupled device camera, and image analysis software (Image-Pro Plus; Media Cybernetics, Silver Spring, MD, USA). Although other pigment pastes (available from Dow Corning) may also be suitable, the red colour chosen for this study was easily detected under the fluorescence microscope.

We also tried injecting a two-component resin (Mercox; Ladd Research, Williston, VT, USA) using a similar injection protocol as for the silicone. This resin had the advantage of being strongly autofluorescent, making it easy to identify filled conduits.

To test whether the silicone or Mercox could pass through end walls we compared the apparent conduit lengths for a range of injection pressure from 0.2 to 1 MPa. If the medium could pass end walls, the apparent length should increase with increasing injection pressure; otherwise the length distribution should be independent of injection pressure.

We followed Cohen's example (Cohen, Bennink & Tyree 2003) in continuing to improve how conduit length distributions are determined from the counts of paint-filled vessels. The traditional 'double-difference' algorithm developed by Zimmermann & Jeje (1981) is based on the raw counts of filled conduits at each stem length. It can yield erratic results, including negative percentages of conduits in some length classes. There is no entirely satisfactory method for handling such results (Tyree 1993). Instead of the double-difference algorithm we fitted an exponential decay function to the declining number  $N_L$  of filled conduits with distance  $L$  from the injection surface

$$N_L = N_0 e^{-kL} \quad (1)$$

where  $N_0$  is the number of conduits at the injection surface, and  $k$  is the best fit extinction coefficient (Cohen *et al.* 2003). Fits were uniformly good, with  $r^2$  generally above 0.9. Assuming random distribution of end walls, the fraction of conduits of length  $L$  ( $P_L$ ) is given by  $L/N_0$  times the second derivative of Eqn 1

$$P_L = Lk^2 e^{-kL}/N_0 \quad (2)$$

Integrating Eqn 2 between two lengths  $L_1$  and  $L_2$  gives the fraction of conduits in that length class ( $P_{LC}$ )

$$P_{LC} = -(1+kL_2)e^{-kL_2} + (1+kL_1)e^{-kL_1} \quad (3)$$

In practice, we represented  $N_L$  by the density of silicone-filled vessels per xylem area rather than counting their total number. Total vessel density did not change systematically along the segments, making this time-saving modification possible. Densities were determined for complete radial sectors of growth rings to ensure correct representation of intra-ring variation in vessel size. In most of the species we were working with current year extension growth and only one growth ring was present.

Most vessels were in the shortest length classes (e.g. Sperry *et al.* 1994), so we used a logarithmic scale to set the lengths for calculating the length distributions

$$L_i = L_{\min}(L_{\max}/L_{\min})^{((i-1)/(n-1))} \quad (4)$$

where  $L_{\min}$  is the shortest non-zero length and  $L_{\max}$  the longest,  $n$  is the total number of lengths, and  $L_i$  is the  $i$ th length counting from  $i = 1$  at  $L_{\min}$ . This scale concentrates the quantification of vessel lengths on the shorter lengths that represent the majority of the vessels. Equation 4 could also be used to set the distances for counting the injected conduits, but in this study these were counted at a subset of the same lengths used in the stem-shortening experiments. We represented the entire vessel length distribution of each species with the mean of the log-transformed length distribution. Length distributions were measured on a minimum of  $n = 5$  stems per species.

For a subset of species (grapevine, willow, boxelder) we also measured the length distribution of vessels separately for different diameter classes ( $n = 5$  stems per species). In this way we could estimate the average diameter of vessels of different lengths. This average diameter was calculated from the average diameter within each diameter class and the fraction of each diameter class in each length class. This method did not account for any tapering in the diameter of a vessel along its length. Taper would cause wide vessels to appear shorter and narrow vessels longer by this method, so it is a conservative measure of differences in diameter versus length relationships.

Tracheid length distributions were handled in the same way except that we used the paint injection method for marking the open conduits. Lengths used for counting the paint-marked tracheids were limited to 1, 2 and 3 mm from the injection surface. Tracheid length distributions were based on averages of  $n = 3$  stems per species.

### Calculation of lumen resistivity ( $R_L$ ) by the Hagen–Poiseuille equation

Cross-sectional areas of conduit lumens were measured in transverse section with the assistance of image analysis software (Image-Pro Plus). Equivalent circle diameters for the lumen cross-sectional area were determined ( $D$ ), and the  $R_L$  calculated as

$$R_L = 128 \eta / (\pi D^4) \quad (5)$$

where  $\eta$  is the viscosity at 20 °C to agree with the direct measurements (0.001 Pa s). All conduits in radial sectors of the secondary xylem were measured (vascular bundles in bracken), and the total  $R_L$  expressed on a xylem area basis ( $\text{MPa s m}^{-2}$ ). In bracken, conductivity was normalized to the area of vascular bundles. The average  $R_L$  per vessel ( $\text{MPa s mm}^{-4}$ ) was determined by multiplying the area-based  $R_L$  by the number of vessels per area. The diameter associated with the average  $R_L$  was calculated by solving Eqn 5 for  $D$ .

Rather than approximating  $D$  as the equivalent circle area it is possible to use equivalent diameters for ellipses

or rectangles inscribed within the vessel lumen (Lewis 1992). The most irregular lumen shapes were observed in bracken. However, when we used the inscribed ellipse method with this species, our estimates of average  $R_L$  did not differ significantly from the equivalent circle approximation. We used the equivalent circle method for all species for consistency and ease of measurement.

### Estimation of end wall resistivity ( $R_W$ )

End wall resistivity on a xylem area basis ( $R_W$ ,  $\text{MPa s m}^{-2}$ ) was calculated assuming lumen ( $R_L$ ) and wall resistivities were in series, summing to equal the total resistivity ( $R_C$ , all on a xylem area basis):

$$R_W = R_C - R_L \quad (6)$$

For the five vessel-bearing species, we estimated  $R_C$  and  $R_L$  from the stem-shortening experiments. The density of open vessels (number of open vessels per xylem area) was estimated for each stem length from the average vessel length distributions assuming random distribution of end walls. A linear regression was fitted to the relationship between  $R$  and density of open vessels ( $r^2 = 0.74\text{--}0.99$ ). The intercept of this regression gave  $R_C = R$  when the density of open vessels is zero. The  $R$  estimate when the density of open vessels equalled the total vessel density gave  $R_L = R$ . This value was compared with the estimate of  $R_L$  from the Hagen–Poiseuille equation to evaluate the validity of this equation for vessel lumens. The  $R_W$  was then calculated from Eqn 6. The wall fraction was  $R_W/R_C$ . For the two tracheid-bearing species, we used the Hagen–Poiseuille equation to estimate  $R_L$ , and  $R_C$  was the average  $R$  of stems longer than the longest tracheid.

All resistivities  $R_W$ ,  $R_C$ ,  $R_L$  could also be expressed on a vessel basis by multiplying them by the average vessel density of the species (converting  $R$  units of  $\text{MPa s m}^{-2}$  to  $\text{MPa s mm}^{-4}$ , the switch to millimetres being for convenience of expression).

In principle, we could also analyse variation in  $R_W$  and  $R_L$  between different vessel size classes within a species. This is a very complex proposition, however, and in this paper we confine ourselves to between-species comparisons of average resistivities.

## RESULTS

### Conduit length distributions

The mean vessel length was always longer using the silicone method than the usual paint pigment method in four species where the methods were compared; the difference was statistically probable in two of the four species (Table 1). The paint either failed to penetrate to the end of the vessels, or did not clearly mark the vessels. We confirmed that the silicone did not penetrate end walls by comparing vessel length distributions in boxelder at different injection pressures ranging from 0.1 to 1 MPa (Fig. 2, solid circles). Mean vessel lengths (log-transformed data) were invariant over

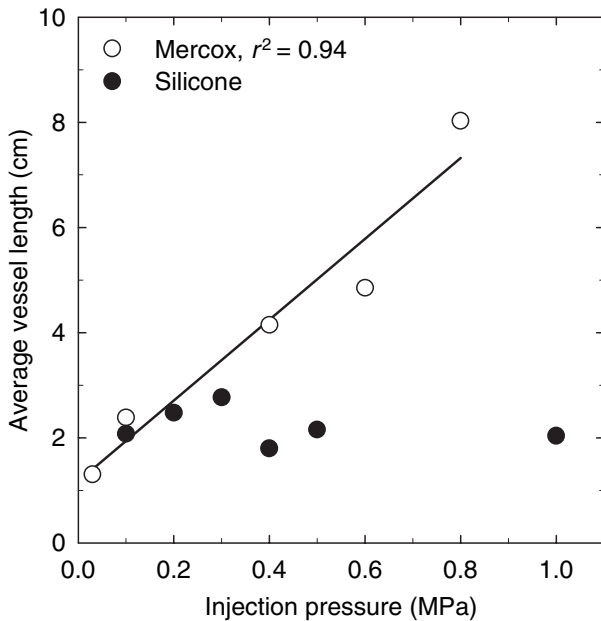


**Figure 2.** Effect of injection pressure on mean vessel length in stems of boxelder (*Acer negundo*). With the silicone method (closed circles) mean vessel length was invariant up to pressures of 1 MPa, indicating the silicone did not penetrate pit membranes. However, Mercocx resin seemed to go through intervessel pit membranes, because mean vessel length was strongly correlated with injection pressure (open circles). Means correspond to log-transformed vessel length distributions.

the entire pressure range suggesting the silicone penetration was stopped by end walls and was not pressure-dependent. In contrast, the same test with Mercocx resin resulted in mean vessel length increasing with injection pressure (Fig. 2, open circles) suggesting this resin penetrated the pit membranes in this species. These results indicated that sil-

icone provided better penetration and identification of vessels than the paint pigment suspension while not crossing end walls like Mercocx. For this reason, further results are reported for the silicone method in the vessel-bearing species.

According to the vessel length distributions in Fig. 3, grapevine had the longest mean vessel length of  $12.8 \pm 4.8$  cm, and willow the shortest at  $1.49 \pm 0.46$  cm. Intermediate were boxelder ( $2.21 \pm 0.35$  cm), bracken ( $2.51 \pm 0.37$  cm), and elderberry ( $3.07 \pm 0.61$  cm; grand mean  $\pm$  SD of  $n \geq 5$  log-transformed distributions). Tracheids, of course, averaged much shorter in ginkgo ( $0.140 \pm 0.002$  cm) and peppertree ( $0.099 \pm 0.023$  cm; grand mean  $\pm$  SD of  $n = 3$  log transformed distributions).

We observed little difference in the average vessel diameter across different length classes in boxelder, grapevine and willow (Fig. 4), although there was a tendency for the shortest length class to have the smallest average diameter.

### Stem-shortening experiments

Initial results showed a decrease in hydraulic resistivity as stems were shortened from 10 cm with the exception of the two shortest lengths (0.3, 0.6 cm) where it tended to increase (data not shown). This is similar to the earlier result of Chiu & Ewers (1993) with *Lonicera fragrantissima*, although they never saw a significant decrease in resistivity, only an increase, as stems were shortened. In our species, we found this increase in resistivity in the shortest segments to result from the hose clamps used to seal the segments to the tubing. This error was particularly severe in species with a large pith and where the current-year's extension growth was used (e.g. elderberry, grapevine). When segments were gently glued in place with cyanoacrylate glue (Krazy Glue; Aron Alpha, Columbus, OH, USA), resistivity showed no increase in short segments, but

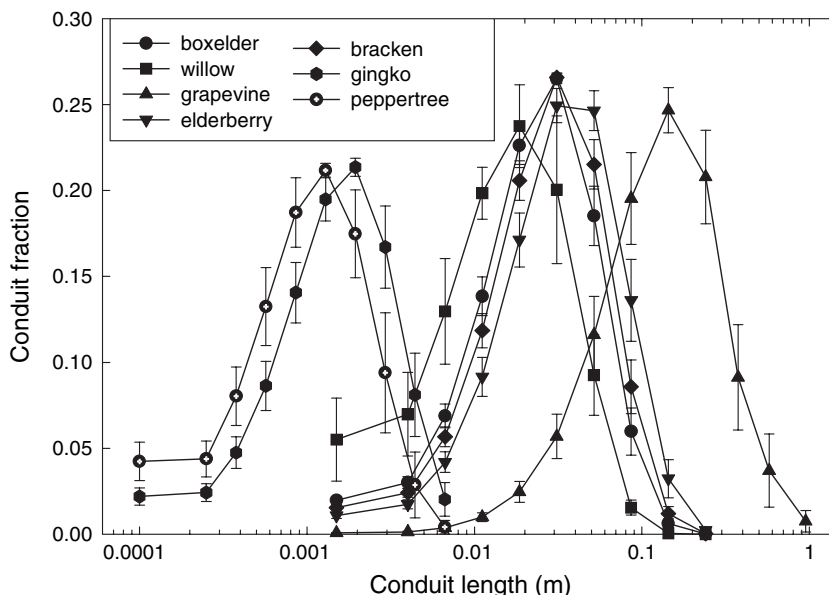


**Figure 3.** Conduit length distributions. Means  $\pm$  SE of  $n \geq 5$  stems for vessel-bearing species, and  $n = 3$  for the two tracheid-bearing species (ginkgo, peppertree).

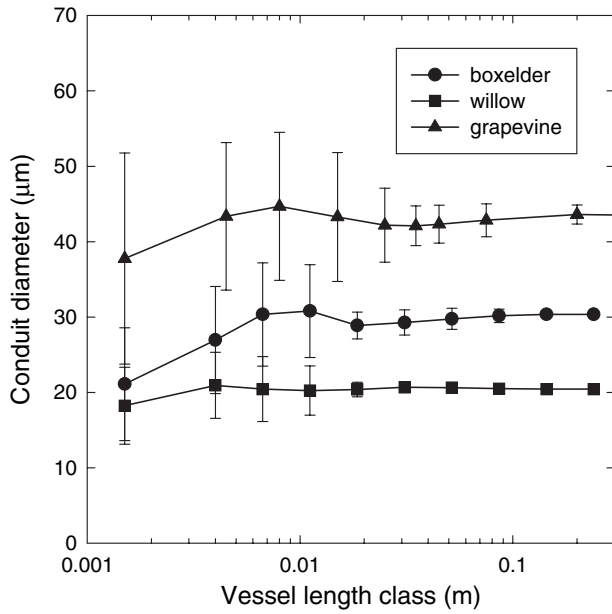


**Figure 4.** Average conduit diameter in vessel length classes for three study species. Means  $\pm$ SD calculated from fraction of vessels of each length class that fell in separate diameter classes.

decreased monotonically as segments were shortened (Fig. 5a). The hose clamps were apparently crushing vessels at the segment end, which was having an increasing effect on segment resistivity as the crushed portion of the flow path became an increasingly greater proportion of the length of the shorter stems.

Using the gluing method we found that the resistivity declined by 35–66% in all vessel-bearing species as stems were shortened from 10 to 0.3 cm (Fig. 5a). This corresponded to an approximately linear decrease in resistivity with increasing density of open vessels at each segment length (Fig. 5b). The resistivity of the xylem without any open vessels ( $R_C = y$  intercept of the regression) spanned three orders of magnitude from a minimum of 48 MPa s m<sup>-2</sup> in grapevine to a maximum of 8890 MPa s m<sup>-2</sup> in peppertree. The resistivity of the xylem with 100% open vessels ( $R_L = y$ -value of regression at total vessel density—dashed extensions in Fig. 5b) showed a similarly broad range from a minimum of 29 MPa s m<sup>-2</sup> in grapevine to a maximum of 6130 MPa s m<sup>-2</sup> in peppertree. The  $R_L$  from the regression was not significantly different from the  $R_L$  calculated from the Hagen–Poiseuille equation (Fig. 5b, open symbols) for any vessel-bearing species ( $t$ -test,  $P < 0.05$ ).

In contrast to the vessel-bearing species, shortening the tracheid-bearing stems caused no significant change in resistivity (Fig. 5a, ginkgo and peppertree). This was consistent with an insignificant number of tracheids being opened at the shortest practicable segment length of 0.3 cm. We calculated the lumen resistivity ( $R_L$ ) for the tracheid-bearing species from the Hagen–Poiseuille equation, a practice suggested by the close agreement seen between calculated and estimated  $R_L$  in the vessel-bearing species.

### End wall resistivity ( $R_W$ ) and conduit allometry

The resistivity of the end walls ( $R_W = R_C - R_L$ ) showed a 1 : 1 proportionality to the lumen resistivity ( $R_L$ ) across the five orders of magnitude range encompassing all species (Fig. 6,  $r^2 = 0.96$ ). The fraction of total resistivity in the end walls ( $F = R_W/R_C$ ) averaged  $0.54 \pm 0.07$  (range 0.31–0.76, values as percentages in Fig. 6). The  $R$ -values in Fig. 6 are expressed on a per conduit basis (MPa s mm<sup>-4</sup>) and so rep-

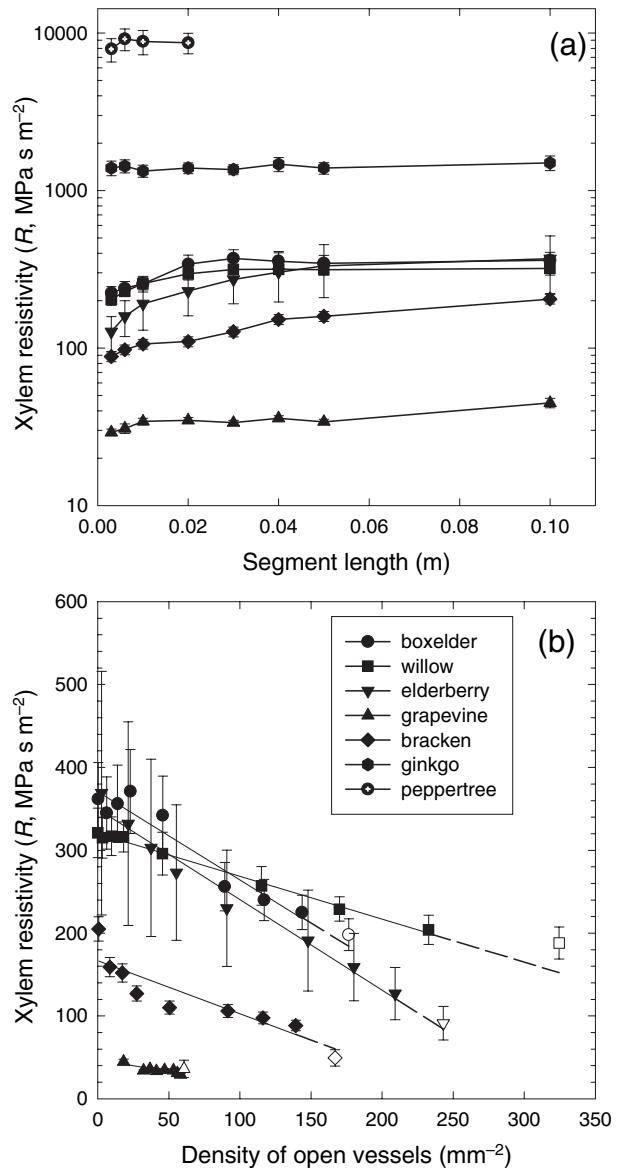


**Figure 5.** (a) Resistivity on xylem area basis ( $R$ ) versus segment length. Means  $\pm$ SE for  $n \geq 10$  segments per species. Resistivities shown on a log scale owing to the three-order-of-magnitude range. (b) Resistivity as in (a) (but linear scale) versus density of open vessels. Open vessels were calculated from segment lengths using the average vessel length distribution of each species. Regressions were extended to 100% open vessels (dashed extensions) to give the estimated lumen resistivity ( $R_L$ ). This corresponded well with the Hagen–Poiseuille lumen resistivity calculated from conduit diameters (open symbols for each species, mean  $\pm$  SE,  $n \geq 4$  stems).

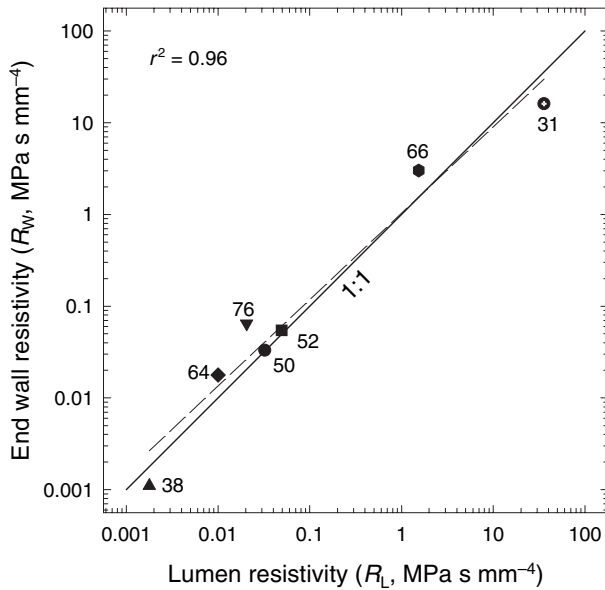


**Figure 6.** Wall ( $R_w$ ) versus lumen resistivity ( $R_L$ ) on a per conduit basis. Regression ( $r^2 = 0.96$ ) is indistinguishable from 1 : 1 line consistent with end wall resistivity averaging near 50% (end wall resistivity percentages given next to symbols, mean =  $54 \pm 7\%$ ). Species symbols as in Fig. 5.

resent variation in conduit size between species. Thus, across diverse species and conduit sizes,  $R_w \approx R_L$ , and end walls accounted for roughly half of the resistivity in the xylem.

Across species, the average conduit length ( $L$ ) was strongly correlated with diameter ( $D$ ; Fig. 7) taking the form of  $L = kD^a$ , where  $k$  is a proportionality constant. The exponent  $a$  for the best fit was 2.02 ( $r^2 = 0.94$ ; Fig. 7, solid regression line). When  $a$  was set to 2, the fit was indistinguishable ( $r^2 = 0.94$ , Fig. 7, dashed regression line on top of solid line), and we conclude that across these species the conduit length scaled with the diameter squared ( $L \propto D^2$ ).

Because the data indicate that on average  $R_w \approx R_L$  (Fig. 6) and that  $L \propto D^2$  (Fig. 7) algebraic relationships (Appendix) mean that the end wall resistance ( $r_w$ ) was inversely proportional to conduit length:

$$r_w \propto 1/L \tag{7}$$

The longer the conduit, the lower the wall resistance. This makes intuitive sense because longer conduits could have longer regions of end wall overlap with more pits. One might expect that the end wall area would be more closely related to its resistance than length alone. However, if the end wall area scaled with total conduit wall area this would require  $L \propto D^{3/2}$  (Lancashire & Ennos 2002), which was not observed (Fig. 7).

Equation 7 also indicates that the product  $r_w L$  is approximately constant, or at least did not vary systematically, across our species. Together with the assumption that  $R_w \propto r_w/L$ , this means that  $R_w/L^2$  is also constant. Using this constant ( $R_w/L^2 = K$ ), an equation linking  $L$  and  $D$  (both in mm) can be derived (Appendix):

$$L = [(\pi K / (128 \eta)) (1/F - 1)]^{0.5} D^2 \tag{8}$$

where  $F$  is the wall fraction ( $R_w/R_C$ ), and  $\eta$  is viscosity in MPa s. The quantity in brackets is the proportionality constant from the  $L \propto D^2$  regression in Fig. 7. Using  $F = 0.54$  (average for data set) yields  $K = 15.5$  MPa s  $\text{mm}^{-2}$ . If we set  $F = 0.05$ , we obtain the length that conduits must achieve to drop the end wall resistivity to 5% of the total resistivity – the ‘compensating length’ shown in Fig. 1. This requires an approximately 4.5-fold increase in conduit length (Fig. 7, dashed 5% wall resistivity line).

## DISCUSSION

The results answered our opening question: on average, lumen and end-wall resistivities were co-limiting (Fig. 6) with approximately 50% of the xylem flow resistance in each component (Fig. 1, co-limiting length). Furthermore, across species conduit length scaled with diameter squared (Fig. 7), meaning that wall resistance was inversely proportional to conduit length. This is consistent with the number of end wall pits being proportional to conduit length rather than being constant or related to conduit wall area. Although these conclusions come from only seven species, they represent most of the range in conduit dimensions in plants.

Earlier conclusions of negligible end wall resistivity in vessel-bearing plants were based on stem-shortening exper-

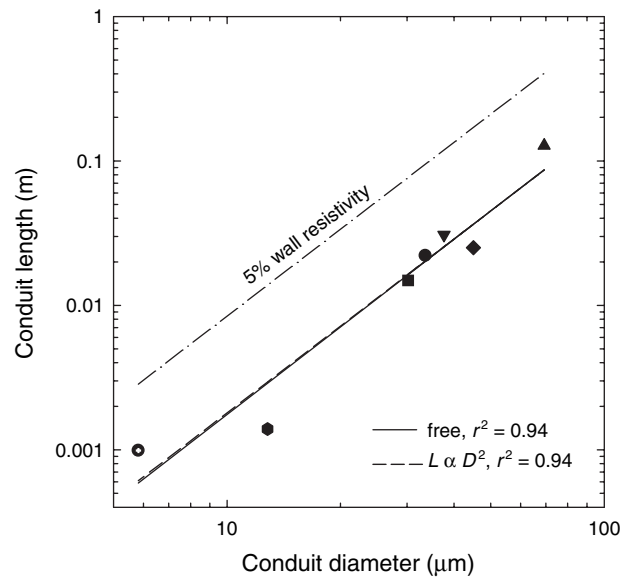


**Figure 7.** Average conduit length ( $L$ ; mean of log transformed data,  $n \geq 3$  stems per species) versus average conduit diameter ( $D$ ). The diameter corresponds to the average lumen resistivity for the species. Species symbols as in Fig. 5. Solid line regression is unconstrained, dashed regression line assumes  $L$  is proportional to  $D^2$ , and overlays the solid line. The complete  $L \propto D^2$  expression is Eqn 8 in text. Upper dashed line corresponds to a 5% end wall resistivity where  $F = 0.05$  in Eqn 8. Conduits must be approximately 4.5 times longer to achieve 5% versus the observed 50% resistivity percentage.

iments in *Lonicera* that did not show a decrease in resistivity with end wall removal (Chiu & Ewers 1993). This contrasts with our data for vessel-bearing species (Fig. 5a). We found it essential to avoid any clamping of the material to avoid crushing the vessels at the point of stem attachment. We observed an increased resistivity in shorter segments as a result of clamping in initial experiments. By avoiding it through gluing stems in place we observed a monotonic decrease in resistivity with end wall removal. Our results for grapevine agree with Lovisolo & Schubert (1998) who found higher conductivities in 0.5-m-long shoot portions of grapevine than in 1.5-m-long segments and attributed the rise in conductivity to the removal of end walls.

We found good agreement between our estimates of lumen resistivity based on hydraulic measurements and Hagen–Poiseuille resistivities calculated from anatomical measurements of conduit diameter (Fig. 5b), thus validating the equation for conduit lumens. This is in agreement with previous measurements on *Fraxinus americana*, a species with simple perforation plates (Zwieniecki, Melcher & Holbrook 2001). In this species, the longitudinal conductivity of single vessels open at both ends agreed well with the Hagen–Poiseuille value. The only species in our study with predominately scalariform perforation plates was bracken (Carlquist & Schneider 1997), and it also was the only species where the Hagen–Poiseuille  $R_L$  was below the estimate from the regression line (Fig. 5b, compare dashed line versus open symbol), although this was not statistically significant. Typical scalariform perforation plates have been found to add approximately 2–6% to the lumen resistivity (Schulte & Castle 1993a; b; Ellerby & Ennos 1998) and we would expect them to cause slight under-estimation of  $R_L$  with the Hagen–Poiseuille equation.

We suspect that some of the previously reported variation in the relationship between Hagen–Poiseuille resistivity and measured resistivity resulted from variation in the number of open vessels in the segments. Vine species (including *Vitis vinifera*), for example, have been reported to have a measured resistivity approaching the Hagen–Poiseuille value (Zimmermann 1983), but our results indicate this was an artefact of measuring the resistivity in segments with a significant number of open vessels. Assuming a linear relationship between the percentage of open vessels and the resistivity (Fig. 5b), a measured resistivity ( $R$ ) in the presence of a known percentage of open vessels (%O) can be corrected to the true value ( $R_C$ ) as long as the lumen resistivity ( $R_L$ ) is also known from the Hagen–Poiseuille equation:  $R_C = (100R - \%OR_L)/(100 - \%O)$ .

The silicone method was superior to the paint method for measuring conduit lengths. Silicone tended to give longer mean vessel lengths than paint (Table 1), while not penetrating the pit membranes unlike the Mercor resin (Fig. 2). This agrees with a recent study (Tyree *et al.* 2003) concluding that paint failed to enter or mark a substantial fraction of the perfused vessels. This problem is eliminated with the silicone, which entirely fills out the lumen and appears to penetrate the full length of the vessel. This

method is based on Jean-Pierre André's pioneering work on vessel casting (André 2002), except that it does not require the difficult and time-consuming digestion of the wood for obtaining silicone casts. We did not test the silicone method for the tracheid-bearing species, and it is unknown whether the silicone would penetrate the large margo pores in many tracheid-bearing gymnosperms at the injection pressure we used (André 2002).

It is an open question why there is such a significant wall limitation in vessel-bearing species where conduit length is at least potentially as long as the plant. We calculated that an approximately 4.5-fold increase in length was necessary to reduce the wall limitation from 50 to 5% (Fig. 7) – from the co-limiting to the compensating length shown in Fig. 1. To achieve this, willow would have to increase its average vessel length from 1.5 to 6.75 cm, well within the capability of plants as indicated by the 13 cm average length of grapevine (Fig. 3). It is true, however, that the 50% point lies at the inflection point of the conductivity versus length curve (Fig. 1, co-limiting length). At this point, the incremental benefit from increasing conduit length has reached its zenith and starts to diminish. This diminishing return must be balanced against the disadvantage of long conduits. Longer conduits increase the impact of embolism on the overall vascular conductance and also facilitate the spread of vascular pathogens (Zimmermann 1983; Comstock & Sperry 2000). Increased conduit size may also result in greater vulnerability to cavitation, although the evidence for this is equivocal (Tyree, Davis & Cochard 1994). Such a relationship would presumably require a link between air-seeding pressure through pits and the total conduit size. Trade-offs between conduit size and safety may result in selection for co-limiting conductivities of lumen and end-wall.

Variation in cavitation resistance may tend to disrupt the  $r_w \propto 1/L$  relationship (Eqn 7) and create more scatter in the  $L \propto D^2$  relationship (Fig. 7). If the resistance of individual pits must increase to prevent air-seeding (Sperry & Hacke 2004), the end wall resistance per conduit length may be greater in more cavitation-protected species unless compensated for by increased end wall overlap. The xylem pressure causing a 50% drop in conductivity by cavitation was relatively similar in the study species, ranging from –0.76 to –3.1 MPa (with the exception of peppertree which has not been measured: Sperry & Hacke 2004; Hacke *et al.* 2004; unpubl. data). Whether the allometry we observed in our limited survey is preserved across a wider range of cavitation resistance remains to be seen.

Our modelling also suggested that vessels should be long enough to minimize the wall resistivity fraction based on estimated wall resistances. For example, we calculated that a vessel 40  $\mu\text{m}$  in diameter would need to only be 1 cm long to reduce end wall resistivity to 5% (Sperry & Hacke 2004). In the present study, a vessel of this diameter was 3 cm long with 50% end wall resistivity, and to reduce this to 5% required a vessel 13.5 cm long (Fig. 7). Our modelling apparently under-estimated the wall resistance either by over-estimating the number of end wall pits per vessel

(50% of total wall area was assumed to be in overlapping end walls) or by under-estimating the resistivity of individual pits (modelled from air-seed pressure and membrane mechanics).

Unresolved is how the end wall fraction varies between length classes *within* a single stem. Our method determined average values for all vessels of a stem, comparing these across different species. The observation that  $L$  was approximately independent of  $D$  within a stem (Fig. 4) but proportional to  $D^2$  across species (Fig. 7) suggests that different scaling relationships occur within a stem. It is theoretically possible to calculate length-class-specific wall fractions from the  $R$  versus open vessel relationships in Fig. 5b. However, the large number of vessels and length classes in a single stem make the influence of end wall resistivity on these data very subtle and thus intractable to analysis.

## ACKNOWLEDGMENTS

Funding was provided from National Science Foundation grants IBN-0112213 and IBN-0416297. We thank Robert Marc and Ann Torrence of Salt Lake City for permission to harvest their grapevine. Jarmila Pittermann helped by collecting peppertree in New Zealand.

## REFERENCES

- André J.-P. (1998) A study of the vascular organization of bamboos (Poaceae-bambuseae) using a microcasting method. *IAWA Journal* **19**, 265–278.
- André J.-P. (2002) *Organisation Vasculaire Des Angiospermes: une Vision Nouvelle*. INRA, Paris, France.
- Carlquist S. & Schneider E.L. (1997) SEM studies on vessels in ferns. 2. Pteridium. *American Journal of Botany* **84**, 581–587.
- Chiu S.T. & Ewers F.W. (1993) The effect of segment length on conductance measurements in *Lonicera fragrantissima*. *Journal of Experimental Botany* **44**, 175–181.
- Cohen S., Bennink J.P. & Tyree M.T. (2003) Air method measurements of apple vessel length distributions with improved apparatus and theory. *Journal of Experimental Botany* **54**, 1889–1897.
- Comstock J.P. & Sperry J.S. (2000) Tansley review, 119. Some theoretical considerations of optimal conduit length for water transport in plants. *New Phytologist* **148**, 195–218.
- Ellerby D.J. & Ennos A.R. (1998) Resistances to fluid flow of model xylem vessels with simple and scalariform perforation plates. *Journal of Experimental Botany* **49**, 979–985.
- Ewers F.W. & Fisher J.B. (1989) Techniques for measuring vessel lengths and diameters in stems of woody plants. *American Journal of Botany* **76**, 645–656.
- Hacke U.G., Sperry J.S. & Pittermann J. (2004) Analysis of circular bordered pit function. II. Gymnosperm tracheids with torus-margo pit membranes. *American Journal of Botany* **91**, 386–400.
- Hargrave K.R., Kolb K.J., Ewers F.W. & Davis S.D. (1994) Conduit diameter and drought-induced embolism in *Salvia mellifera* Greene (Labiatae). *New Phytologist* **126**, 695–705.
- Kolb K.J. & Sperry J.S. (1999) Differences in drought adaptation between subspecies of sagebrush (*Artemisia tridentata*). *Ecology* **80**, 2373–2384.
- Lancashire J.R. & Ennos A.R. (2002) Modelling the hydrodynamic resistance of bordered pits. *Journal of Experimental Botany* **53**, 1485–1493.
- Lewis A.M. (1992) Measuring the hydraulic diameter of a pore or conduit. *American Journal of Botany* **79**, 1158–1161.
- Louden C. & McCulloh K.A. (1999) Application of the Hagen–Poiseuille equation to fluid feeding through short tubes. *Annals of the Entomological Society of America* **92**, 158–158.
- Lovisolo C. & Schubert A. (1998) Effects of water stress on vessel size and xylem hydraulic conductivity in *Vitis vinifera* L. *Journal of Experimental Botany* **49**, 693–700.
- Martre P., Cochard H. & Durand J.L. (2001) Hydraulic architecture and water flow in growing grass tillers (*Festuca arundinacea* Schreb.). *Plant, Cell and Environment* **24**, 65–76.
- Schulte P. & Castle A. (1993a) Water flow through vessel perforation plates – effects of scalariform plate angle and thickness. *Journal of Experimental Botany* **44**, 1143–1148.
- Schulte P.J. & Castle A.L. (1993b) Water flow through vessel perforation plates – a fluid mechanical approach. *Journal of Experimental Botany* **44**, 1135–1142.
- Schulte P.J. & Gibson A.C. (1988) Hydraulic conductance and tracheid anatomy in six species of extant seed plants. *Canadian Journal of Botany* **66**, 1073–1079.
- Sperry J.S. & Hacke U.G. (2004) Analysis of circular bordered pit function. I. Angiosperm vessels with homogenous pit membranes. *American Journal of Botany* **91**, 369–385.
- Sperry J.S., Nichols K.L., Sullivan J.E.M. & Eastlack S.E. (1994) Xylem embolism in ring-porous, diffuse-porous, and coniferous trees of northern Utah and interior Alaska. *Ecology* **75**, 1736–1752.
- Tyree M.T. (1993) Theory of vessel-length determination: The problem of nonrandom vessel ends. *Canadian Journal of Botany* **71**, 297–302.
- Tyree M.T. & Ewers F.W. (1991) Tansley review, 34: The hydraulic architecture of trees and other woody plants. *New Phytologist* **119**, 345–360.
- Tyree M.T., Cochard H. & Cruiziat P. (2003) The water-filled versus air-filled status of vessels cut open in air: the ‘Scholander assumption’ revisited. *Plant, Cell and Environment* **26**, 613–621.
- Tyree M., Davis S. & Cochard H. (1994) Biophysical perspectives of xylem evolution – Is there a tradeoff of hydraulic efficiency for vulnerability to dysfunction? *IAWA Journal* **15**, 335–360.
- Zimmermann M.H. (1983) *Xylem Structure and the Ascent of Sap*. Springer-Verlag, Berlin, Germany.
- Zimmermann M.H. & Jeje A.A. (1981) Vessel length distribution of some American woody plants. *Canadian Journal of Botany* **59**, 1882–1892.
- Zwieniecki M.A., Melcher P.J. & Holbrook N.M. (2001) Hydraulic properties of individual xylem vessels of *Fraxinus americana*. *Journal of Experimental Botany* **52**, 257–264.

Received 19 August 2004; received in revised form 18 October 2004; accepted for publication 19 October 2004

## APPENDIX

### Derivation of Eqn 7

The  $R_L \propto 1/D^4$  according to the Hagen–Poiseuille equation. Because  $R_W \approx R_L$  (Fig. 6),  $R_W \propto 1/D^4$ . The  $R_W \propto r_W/L$  assuming that the length between tapered end walls of a vessel is proportional to the vessel length. Substituting this proportionality for  $R_W$  means that  $r_W \propto L/D^4$ . Further substituting the observation that  $D \propto L^{0.5}$  (Fig. 7) leads to  $r_W \propto L/L^2$  which reduces to Eqn 7.

**Derivation of Eqn 8**

The wall fraction ( $F$ ) in terms of  $R_w$  and  $R_L$  is:

$$F = R_w / (R_w + R_L) \quad (\text{A1})$$

Assuming the product  $r_w L$  is constant (Eqn 7), and that  $R_w \propto r_w / L$ , the  $R_w = K / L^2$  with  $K$  being a proportionality

constant. Substituting this for  $R_w$  in Eqn A1 and the Hagen–Poiseuille equation for  $R_L$  gives:

$$F = (K/L^2) / (K/L^2 + 128 \eta / (\pi D^4)) \quad (\text{A2})$$

using units of MPa, s, and mm. Solving this for  $L$  as a function of  $D$  yields Eqn 8.